JOURNAL OF VIROLOGY, Dec. 1988, p. 4577–4585
0022-538X/88/124577-09$02.00/0

Vol. 62, No. 12

The Herpes Simplex Virus Latency-Associated Transcript Is Spliced during the Latent Phase of Infection

EDWARD K. WAGNER,[1]* W. MICHAEL FLANAGAN,[1] GAYATHRI DEVI-RAO,[1] YI-FAN ZHANG,[1] JAMES M. HILL,[2] KEVIN P. ANDERSON,[3] AND JACK G. STEVENS[4]

Department of Molecular Biology and Biochemistry, University of California, Irvine, Irvine, California 92717[1]; Department of Microbiology and Immunology, University of California, Los Angeles, Los Angeles, California 90024[4]; Lions Eye Research Laboratories, LSU Eye Center, Louisiana State University Medical Center, New Orleans, Louisiana 70112[2]; and Genentech Inc., 460 Point San Bruno Boulevard, South San Francisco, California 94080[3]

Received 1 April 1988/Accepted 12 August 1988

The herpes simplex virus type 1 latency-associated transcript (LAT) is expressed as a major species 2,100 to 2,200 bases in length and a less abundant one ca. 730 bases shorter in latently infected mouse and rabbit neurons. RNA blot hybridization experiments using 20- to 22-base synthetic oligonucleotides and mung bean nuclease protection assays have demonstrated that the smaller LAT species is colinear with the larger one, except for a 730-base intron. On the basis of Northern blot analysis, the spliced species which comprises as much as 50% of the total LAT in latent infections of mice with several strains of herpes simplex virus type 1 and latent infections of rabbits with either the McKrae or the KOS(M) strains of virus is not present in the acute phase of infection. Further and rather surprisingly, in mice latently infected with the KOS(M) strain of virus, the spliced LAT species is considerably less abundant. This suggests that both the strain of virus and the animal in which the latent infection occurs are important in either the processing or stability of spliced LAT. Finally, an exhaustive series of experiments failed to provide convincing evidence that a unique, poly(A)$^+$ species of LAT exists in the latent phase of infection.

The latent phase of herpes simplex virus type 1 (HSV-1) infection of mice sensory nerve ganglia is distinguished by the transcription of RNA from a single region of the genome. The RNA expressed is partially complementary to the gene encoding the major α regulatory protein ICP0 (19). Since this pattern of transcription has also been observed in human and rabbit latent infections (4, 18a), it seems likely that either the transcript itself or a protein encoded by it will have an important role in the latent state. We have been able to use a mutant of HSV-1 that does not express latency-associated transcripts (LATs) to demonstrate that these are not absolutely required for the establishment of the latent phase of infection in mice (9a).

In order to further investigate the function of HSV-1 LATs, we and others have characterized transcription during the latent phase of infection and have defined a family of expressed transcripts (16, 17, 18a). Almost all HSV-1 LATs have been found to be confined to the nuclei of latently infected neurons, and the large majority can be recovered in the poly(A)$^-$ fraction by using oligo(dT)-cellulose chromatography. Two colinear species of poly(A)$^-$ HSV-1 LATs can be isolated from latently infected mouse sensory nerve ganglia. In our laboratories, using the KOS(M) strain of HSV-1, the larger one is about 2.2 kilobases (kb) in size and represents on the order of 90% of the total LATs recovered. Sequence analysis of the KOS(M) strain of HSV-1 DNA encoding LAT demonstrated the existence of two potential open translational reading frames. Interestingly, however, no consensus polyadenylation signal located in close proximity to the 3′ end of the poly(A)$^-$ LAT species was found (22).

In the present communication, we used RNA from rabbit trigeminal ganglia latently infected with the McKrae strain of HSV-1 to show that the less abundant 1.5-kb LAT species is derived by the splicing of a 730-base intron from the larger one. In both mice and rabbits, the spliced species was not detected in acutely infected ganglia; therefore,processing of the transcript is related to the latent phase of infection.

In rabbits latently infected with McKrae strain virus, the spliced species comprised as much as 50% of the total LATs; this proportion was also seen in RNA isolated from mouse sensory nerve ganglia latently infected with the 17*syn*$^+$, McKrae, and MacIntyre strains of HSV-1. Surprisingly, the amount of spliced LAT recoverable from ganglia latently infected with the KOS(M) strain depended on the animal used. In mice it was no more than 10% of the total LATs seen, while in rabbits it was as much as 50%.

One consequence of the splice is the positioning of the only large open reading frame encoded by LAT significantly closer to the 5′ end of the transcript. Despite such suggestive evidence that LAT could function to encode a protein, we could find no evidence for a separate poly(A)$^+$ species of the HSV LAT.

MATERIALS AND METHODS

Establishment of acutely and latently infected rabbits and processing of trigeminal ganglia. As described previously (7), unscarified corneas of 1.5- to 2.5-kg New Zealand albino rabbits were inoculated with 2×10^6 to 4×10^6 PFU of the McKrae strain of HSV-1 in 25 μl. Primary corneal infection was verified by slit-lamp biomicroscopic examination 4 to 8 days postinoculation. Assay of spontaneous or induced virus shedding was assayed by tear film swab, also as described previously (1). Acutely infected ganglia were taken from rabbits at 7 or 12 days postinfection, and latently infected ones were taken from 60 to 120 days postinoculation. At 3 to 5 days and 1 to 2 h before sacrifice, eyes were swabbed to assay for virus. Ganglia were removed, immediately frozen in liquid nitrogen, and stored at −70°C before extraction of RNA.

* Corresponding author.

Establishment of acutely and latently infected mice and processing of spinal ganglia. As has been described previously (19), 6-week-old outbred, male Swiss-Webster mice (Simonson Laboratories, Gilroy, Calif.) were used in all experiments. The mice were inoculated in each rear foot with 10^7 to 10^8 PFU of nonneuroinvasive HSV-1 KOS(M) or with 10^4 to 10^5 PFU of strains 17*syn*$^+$, McKrae, or MacIntyre. In these latter cases, this dosage corresponds to approximately 1 50% lethal dose for each strain used. The derivation of the KOS(M) strain and methods used for inoculation have been described previously (19, 21). After 4 days (acute infections) or after 3 or more weeks (latent infections), ganglia were dissected from the animals, quick frozen in liquid nitrogen, and either cut on a cryostat or stored at −70°C until use.

RNA isolation and fractionation. RNA was isolated from nerve ganglia and cultured cells by using the guanidinium-isothiocyanate hot phenol method described previously (19, 22, 23). Total (unfractionated) RNA from one latently infected rabbit trigeminal ganglia was sufficient for four to five RNA blots, while a single blot generally required 15 to 20 mouse latently infected lumbosacral spinal ganglia. Less HSV-specific RNA could be recovered from acutely infected ganglia; here RNA from about 50 mouse ganglia or from one complete rabbit trigeminal ganglion was used for a single RNA blot. Rabbit skin cells were grown and infected with 10 PFU per cell of the KOS(M) strain of HSV-1 as described previously (19, 21, 23). When treated with cycloheximide, cells were preincubated for 60 min in the presence of 50 μg of the drug per ml, which was also present at this concentration during virus adsorption and after infection as described previously (23).

Poly(A)$^+$ RNA was selected by oligo(dT)-cellulose (Collaborative Biochemicals) chromatography as has been described previously (6, 22). In order to ensure efficient fractionation, the amount of oligo(dT)-cellulose was increased from the previously used 75 to 125 mg per latently infected rabbit or batch of 50 latently infected mouse ganglia. In several instances, RNA in the poly(A)$^+$ fraction was refractionated by a second passage through a fresh oligo(dT) column. We used the poly(A)$^+$ RNA from one rabbit or from 50 mouse latently infected ganglia for a single RNA blot.

Poly(A)$^-$ or total RNA was extensively digested in a volume of 500 μl with 6 U of RNase-free DNase in DNase buffer containing 400 U of RNasin per rabbit ganglia or batch of 50 mouse ganglia. It was size fractionated by electrophoresis using 1.2% agarose gels containing 6% formaldehyde and was subsequently blotted onto nylon membranes (10) in 20× SSC (1× SSC is 0.15 M NaCl, 0.015 M sodium citrate).

Recombinant DNA and preparation of radiolabeled probes. All recombinant DNA was from the KOS(M) strain of HSV-1; fragments were cloned into pUC vectors as described previously (10, 12). For synthesis of ^{32}P-labeled cloned DNA probes, the HSV-specific DNA fragment was isolated by digestion of the total plasmid with the appropriate restriction enzymes (Bethesda Research Laboratories, Inc., Gaithersburg, Md., or Boehringer-Mannheim Biochemicals, Indianapolis, Ind.) followed by electrophoresis and electroelution. Synthesis of uniformly labeled probes was accomplished by nick translation, using [α-^{32}P]dCTP (3 Ci/μmol; Amersham Corp., Arlington Heights, Ill.) (6, 22). Synthetic oligomer probes were 5′-end labeled to a specific activity of 5×10^5 cpm/ng, using [γ-^{32}P]ATP (7 Ci/μmol; ICN Biochemicals) and bacteriophage T4 kinase (Bethesda Research Laboratories) as described by Maniatis et al. (10). In brief, ca. 50 ng of oligonucleotide was heated to 90°C for 3 min in a 9-μl volume of 20 mM glycine (pH 9.5)–0.1 mM EDTA–1 mM spermidine and quenched on ice. The solution was then adjusted to a final concentration of 50 mM glycine–10 mM $MgCl_2$–5 mM dithiothreitol–5% glycerol, and the kinasing reaction was carried out by standard methods.

Oligo(dT)-primed cDNA was synthesized by using 5 μg of oligo(dT)$_{12-18}$ (Collaborative Bioresearch) and the total or poly(A)$^+$ RNA fraction from one latently infected rabbit trigeminal ganglion. Synthesis of cDNA was carried out with 25 U of reverse transcriptase (Life Sciences, Inc., St. Petersburg, Fla.) in 30 μl of a buffer (pH 8.3) containing 50 mM NaCl, 35 mM Tris, 5 mM $MgCl_2$, and 400 μM deoxyribonucleoside triphosphates lacking dCTP. The cDNA extension mix contained 50 μCi of [α-^{32}P]dCTP, and synthesis was carried out for 30 min at 37°C. The mixture was then treated with RNase A and phenol extracted as described previously (9, 11). The average size of cDNA synthesized in this manner was determined to be 50 to 100 nucleotides based on fractionation of a sample on a denaturing acrylamide gel. This size is similar to that reported previously for similar experiments (8).

Hybridization conditions. RNA transfer blots were hybridized in a volume of 5 ml containing 4×10^7 cpm (Cerenkov) of radiolabeled nick-translated DNA in the presence of 50% formamide–0.4 M Na^+–0.1 M HEPES (*N*-2-hydroxymethylpiperazine-*N*′-2-ethanesulfonic acid) (pH 8.0)–0.005 M EDTA–Denhardt solution containing 100 μg of denatured calf thymus DNA per ml (5) at 49°C for 40 h. Details and procedures for rinsing have been described previously (6, 22). For hybridization with synthetic oligomer probes, the same amount of radioactive DNA was incubated at 48°C in 6× SSC–10× Denhardt solution–0.5% sodium dodecyl sulfate–50 mM Na_2HPO_4 (pH 6.5) for 16 h. Such blots were rinsed with two successive 30-min washes of 3× SSC containing 0.1% sodium dodecyl sulfate at room temperature, one rinse at 48°C, and a final rinse at 8 to 10°C below the T_m of the oligomer (calculated from the formula T_m = 4 [number of G or C residues] +2 [number of A or T residues]). For hybridization with oligo(dT)-primed cDNA, the total radioactivity obtained (between 1.2×10^6 to 4×10^6 cpm) was hybridized to appropriate DNA dot blots at 48°C for 40 h in the same buffer used for nick-translated RNA probes and was rinsed as described.

For mung bean nuclease protection assays, RNA from 20% of a latently infected rabbit trigeminal ganglia or 50 μg of tRNA was incubated with 50 ng of 5′-end-labeled oligonucleotide probe (2.5×10^7 cpm) in 50 μl of a solution containing 100 mM HEPES, 200 mM Na^+, and 5 mM EDTA. The sample was covered with mineral oil, heated to 90°C for 10 min, and then annealed at 70°C for 3 h. After hybridization, 400 μl of a mixture of 50 mM sodium acetate (pH 5), 30 mM NaCl, 1 mM $ZnSO_4$, and 10% glycerol containing 100 U of mung bean nuclease (New England BioLabs, Inc., Beverly, Mass.) was added. At this time 10% was taken as a zero time control; the remainder was incubated for 45 min at 37°C, and an additional 100 U of mung bean nuclease was added. After a further 45 min, 40 μl of a 10× stop buffer was added (1× is 50 mM Tris base (pH 9.5) and 10 mM EDTA). The solution was extracted with phenol and chloroform, and protected material was precipitated by ethanol precipitation and fractionated on denaturing 12% polyacrylamide-urea gels versus the appropriate size standards.

In situ hybridization was carried out with ^{3}H-labeled single-stranded RNA probes. The *Sal*I-*Bcl*I fragment of HSV-1 KOS(M) DNA, spanning bases 1739 through 2975

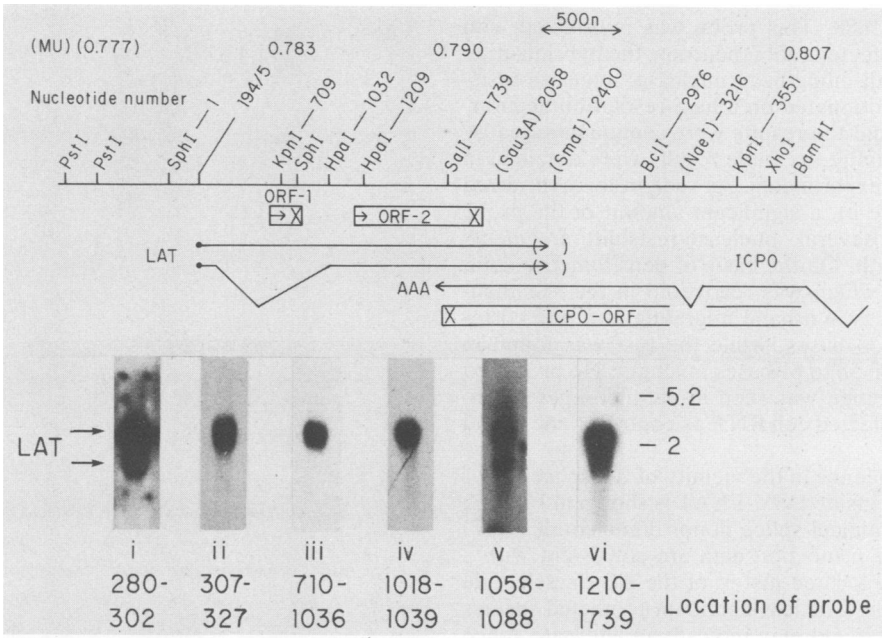

FIG. 1. RNA transfer blot analysis of the unspliced and spliced HSV-1 LAT from latently infected rabbit trigeminal ganglia. The position of HSV-1 LAT on the HSV-1 genome and its relation to the ICP0 gene is based on previously published data (22) and is presented here. RNA from latently infected rabbit ganglia was extracted and fractionated on formaldehyde-containing agarose gels as described in Materials and Methods. The approximate migration positions of 5.2- and 2-kb rRNA size standards are indicated. RNA was hybridized either with cloned viral DNA fragments radiolabeled by nick translation or with defined oligonucleotide probes labeled by kinasing. The positions of the probes are based on the previously published sequence numbers (22).

(see Fig. 1), was cloned between the *Sal*I and *Bam*HI sites of pGEM1 and pGEM2 (Promega Biotec, Madison, Wis.) so that both orientations could be transcribed, using the T7 promoter as described by the supplier. Templates were linearized with *Hin*dIII or *Eco*RI and were purified by agarose gel electrophoresis and electroelution. Transcription experiments were carried out by using 100 μCi each of ^{3}H-labeled UTP, CTP, and ATP (Amersham; 14.1 Ci, 20 Ci, and 32 Ci/mM, respectively). The mix contained 50 mM unlabeled GTP and CTP, and the reaction was accomplished with 5 U of T7 polymerase (Bethesda Bioresearch) according to the instructions of the supplier. DNA templates were removed by digestion with RNase-free DNase (Stratagene) for 30 min at 37°C, and RNA was purified by phenol chloroform extraction. Probes of specific activities of approximately 3×10^7 cpm/μg were obtained by using these standard methods. The RNA probes were then degraded to a size range of 50 to 200 bases as judged by electrophoresis in 9% denaturing polyacrylamide gels and incubation in 100 mM NaOH for 3 h on ice. Probes were reextracted with phenol chloroform, ethanol precipitated, and then used. Sectioning and fixation of tissues, preparation of slides, prehybridization, hybridization, and radioautography were carried out as described earlier (19). Conditions for posthybridization treatment and RNase digestion to remove unhybridized probe were described by Cox et al. (3). Slides were developed after a 2-week exposure, stained with Giemsa, and observed.

RESULTS

HSV-1 LAT is spliced. As discussed previously, a number of features of HSV-1 LAT expression in latently infected neurons suggested to us that the smaller poly(A)$^-$ RNA might be a spliced product of the major transcript (22). The data shown in Fig. 1 demonstrate that this is the case. In this experiment, total RNA isolated from rabbit trigeminal nerve ganglia latently infected with the McKrae strain of HSV-1 was fractionated on formaldehyde-containing agarose gels, blotted onto nylon membranes, and hybridized with short radioactive DNA probes spanning the portion of the HSV-1 genome encoding LAT. We chose this method of analysis to maximize the resolution obtainable from a limited source of RNA. Nucleotide numbers for the positions of these probes are from the published sequence (22), which extends from the *Sph*I site at 0.780 to a *Sma*I site at 0.795 map units. Numbers beyond this site (base 2400) are based on data presented in this report (see below).

Probes between the cap site (base 195) and base 301 of the sequence of the DNA encoding the LAT hybridized to both unspliced (2.2 kb) and spliced species (1.5 kb), as did probes beyond base 1058 (Fig. 1, lanes i, v, and vi). In contrast, probes between these two sites hybridized only to the larger, unspliced LAT (lanes ii to iv). Our hybridization criteria and rinse were such that an oligonucleotide with less than a 16- to 18-base homology could not hybridize with cRNA. Since oligonucleotide probes spanning bases 307 to 327 and 1018 to 1039 hybridized only to unspliced LAT (lanes ii and iv), the 5′ limit of the intron is placed between bases 297 to 314 and the 3′ limit is between bases 1020 and 1058.

The fact that all the oligonucleotide probes used in this region of the LAT gene hybridized to the larger, unspliced species of LAT served as an internal control demonstrating the high homology between the sequence of the KOS(M) strain of HSV-1 used to synthesize the probes and the McKrae strain of virus. We confirmed the resolution of the oligonucleotide-mapping data by carrying out a nuclease protection assay to precisely locate the splice acceptor site. Here we used a 5′-end-labeled 71-base oligomer spanning

bases 1018 through 1088. This probe was hybridized with RNA from latently infected rabbit neurons, the hybridization mix was digested with mung bean nuclease, nuclease-resistant material was fractionated on a high-resolution denaturing acrylamide gel, and the results were semiquantitated by densitometry. Essentially the same results were obtained in several independent experiments. As seen in the hybridized sample (Fig. 2A, lane ii), a significant amount of the probe was recovered in several nuclease-resistant fragments smaller than full length. On the basis of densitometric data, 70% of the material which was recovered in the less-than-full-length fraction was in a band migrating at a rate corresponding to that of 53 bases, while the rest was found in products ranging from 58 to 61 bases in length. No protected species in this size range was seen in parallel digests containing tRNA or uninfected cell RNA as controls (lane iv and not shown).

The nucleotide sequence in the vicinity of the splice donor and acceptor regions inside HSV-1 LAT is shown in Fig. 2B. Several potential canonical splice donor dinucleotides (GT) are shown. Nuclease protection data are consistent with a splice acceptor being located just 3′ of the AG dinucleotide at bases 1033 and 1034. The less-abundant protected species were consistently seen and may indicate an alternate splice acceptor near base 1028 or incomplete digestion by the mung bean nuclease. The position of the splice acceptor or acceptors is within the sequence of the oligonucleotide probe which only hybridized to the unspliced species (Fig. 1, lane iv).

Splicing of LAT species appears to be specific to latently infected neurons. As discussed previously (19), latent HSV infection in mouse sensory nerve ganglia occurs after an acute period of infection. Genes related to lytic cycle functions are transcribed during this acute phase of infection but become undetectable by 7 days after footpad inoculation of mice. During this acute period of infection, nuclear LAT is also expressed and is readily detectable by in situ hybridization. An illustration of the differences between acute and latent phases of infection can be seen by analysis of transcription of LAT compared with a lytic phase α transcript, ICP0. An example, using strand-specific in situ hybridization probes for LAT and ICP0, is shown in Fig. 3. Here, ICP0 is seen only in the lytic phase, LAT is detected in both lytic and latent phases.

In order to investigate the relationship between degree of splicing and stage of infection, we carried out Northern (RNA) blot analyses of LATs from acutely and latently infected ganglia. Acutely infected ganglia are technically difficult to deal with because of the active virus infection and inflammatory response taking place, however sufficient material could be isolated for analysis. As seen in Fig. 4A (lane i), spliced LAT was below the limits of detection in rabbit ganglia taken 7 days after eye inoculation with the McKrae strain of HSV-1, a time when infectious virus is still detectable. By 12 days postinoculation, small amounts of the spliced transcript (ca. 5 to 10% of the total LAT) were seen (Fig. 4B, lane ii). In mice latently infected with the KOS(M) strain of HSV-1, the proportion of spliced LAT is less than that seen in rabbits infected with McKrae virus (Fig. 4, lane iv); however, the spliced LAT species was not detectable in RNA isolated from virus containing mouse ganglia isolated 4 days after footpad inoculation (Fig. 4, lanes v and vi).

Finally, we assayed LAT expressed during productive infection of rabbit skin cells and found results similar to those seen with RNA from the acute phase of infection in animals. As noted previously (19), LAT is expressed at low

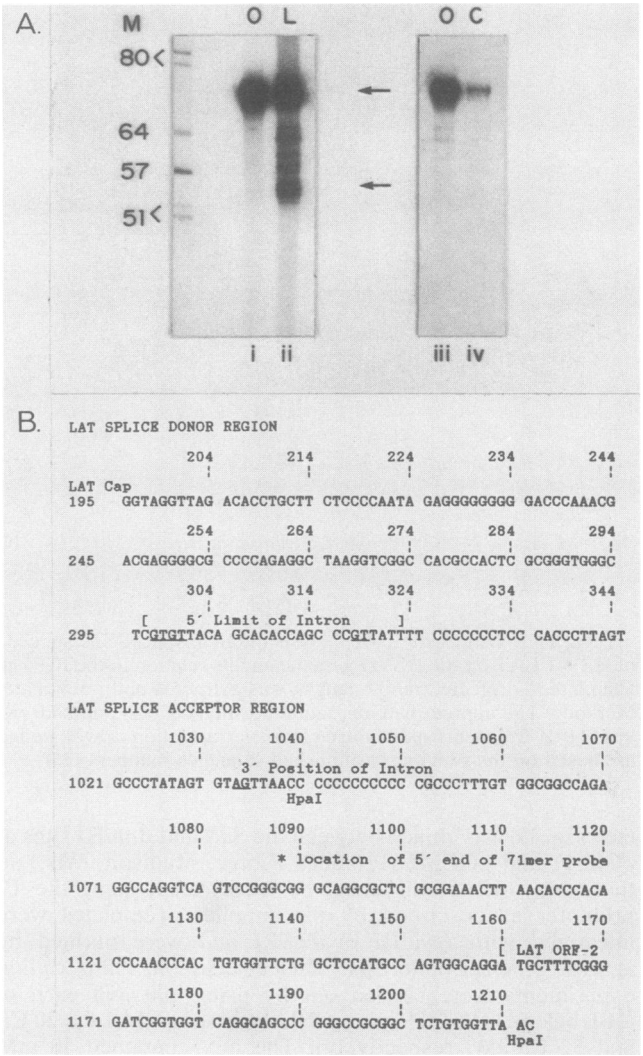

FIG. 2. (A) Precise localization of the splice acceptor for HSV-1 LAT. lane L contains mung bean nuclease-resistant material from the hybridization of RNA from 20% of a rabbit trigeminal ganglia latently infected with the McKrae strain of HSV-1, and lane C contains only tRNA as a control. Nuclease-resistant material was fractionated on a 12% denaturing acrylamide-urea gel run as described previously (22). Lane M contains size markers obtained by end labeling *Hae*III-digested pBR322 DNA. Lanes 0 are zero-time controls (see Materials and methods). (B) Positions of the splice donor and splice acceptor regions for HSV-1 LAT. The data from Fig. 1 were correlated with the LAT gene sequence as described in the text. The 3′ end of the intron is situated between bases 297 and 314, since probes to the left of base 301 hybridize to both spliced and unspliced LAT while those to the right hybridize only to the unspliced species. Similarly, the 3′ end is located between bases 1020 and 1058 by oligonucleotide mapping, while the data of panel A places it near base 1033. Potential GT dinucleotides for the beginning of the intron and the AG dinucleotide demarking the end are underlined.

abundance in infected cultured rabbit skin cells. Although a complete analysis will be detailed elsewhere (E. K. Wagner, Y.-F. Zhang, W. M. Flanagan, R. Javier, F. Sederati, and J. G. Stevens, manuscript in preparation), it should be noted that LAT can be quantitatively recovered in the poly(A)$^-$ fraction from cells 3 to 6 h after infection either in the presence or absence of cycloheximide, and there is no

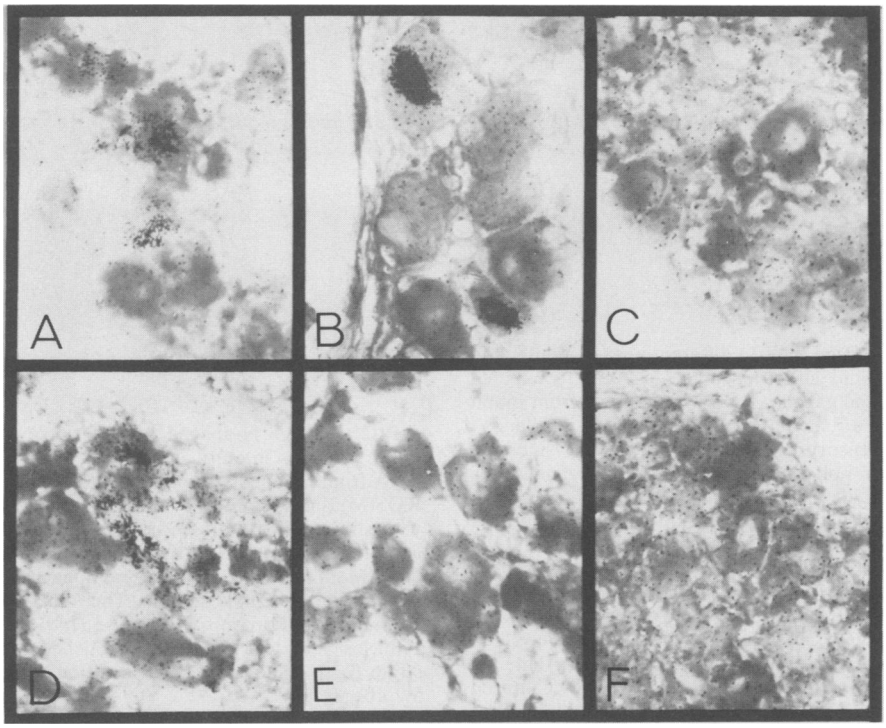

FIG. 3. Murine spinal ganglia probed for expression of HSV-1 LAT and ICP0, using strand-specific RNA probes. Panels A, B, and C show ganglia hybridized with in vitro-synthesized ^{3}H-labeled RNA probe specific for LAT; panels D, E, and F show ganglia hybridized with probe specific for ICP0. Ganglia in panels A and D are acutely infected, note grains over neuronal nuclei, cytoplasm, and outside cells. Panels B and E show latently infected ganglia, note that only panel B (LAT RNA probed) shows hybridization, and this is essentially nuclear. Panels C and F are from uninfected controls. Experimental details are described in the Materials and Methods section. Magnification, ×300.

evidence of a spliced species. An example of a Northern blot of RNA isolated from such cells is shown in Fig. 4B. Here, we hybridized cloned, radiolabeled DNA spanning the *Sph*I site at base 1 to the *Kpn*I site at base 709 with RNA from either cycloheximide-treated or untreated cells infected with the KOS(M) strain of HSV-1 (lanes i and ii). For comparison, we included a sample of RNA from rabbit ganglia latently infected with the McKrae strain of virus (lane iii). It is clear that no detectable LAT migrating with the size expected for the spliced species was seen.

The presence of a significant amount of spliced LAT in rabbits was not correlated with periods of induced or spontaneous reactivation of the virus. Thus, the proportion of spliced LAT was not consistently different in RNA from ganglia which were isolated as many as 100 days or as few as 3 days after a measured spontaneous or induced reactivation. For example, the RNA shown in lane i of Fig. 1 was isolated from ganglia 5 days after the detection of virus in the tear film, whereas that shown in lane v was recovered from ganglia isolated 90 days after the last detection of virus.

Efficiency of splicing of LAT in the latent phase of infection depends on both the animal and the strain of virus used. As was shown above, there is a significant difference in the relative amount of the spliced species of LAT recovered from mice latently infected with the KOS(M) strain of HSV-1 compared with that recovered from rabbits infected with the McKrae strain. Therefore, we compared the proportion of spliced LAT seen in mouse sensory nerve ganglia latently infected with the McKrae, 17*syn*$^+$, and MacIntyre strains of HSV-1 with that from mice and rabbits infected with the KOS(M) strain. We hybridized the blots with cloned, radiolabeled DNA spanning the *Hpa*I site at base 1210 to the *Sal*I site at base 1740 in order to avoid problems with small sequence divergences among strains. On the basis of densitometric measurements, the amounts of spliced species ranged from 40 to 50% of the total LATs from mice latently infected with the McKrae, 17*syn*$^+$, and MacIntyre strains (Fig. 5, lanes i, ii, and iv), while it was typically in the range of 5 to 10% of the total in mouse sensory nerve ganglia latently infected with the KOS(M) strain of HSV-1 (lanes iii and v). Quite surprisingly, RNA from the trigeminal ganglia of rabbits latently infected with the KOS(M) strain yielded a proportion of spliced LATs equivalent to that seen with other strains of virus (lane vi).

These data suggest that both the strain of HSV-1 used and the animal in which the latent infection is established affect the amount of spliced LATS which can be recovered from neurons. This result could be due to either a difference in the efficiency of splicing in the different systems or a difference in the stability of spliced LAT in mouse sensory nerve ganglia latently infected with the KOS(M) strain of HSV-1. In either case, differences in the DNA sequences encoding LATs must be an important factor in these differences between strains of virus. A comparison of the sequences between the KOS(M) and 17*syn*$^+$ strains of virus was detailed previously (22), and recently the full sequence of the long repeat region of the latter strain has been made available (L. Perry and D. McGeoch, submitted for publication). The KOS(M) strain of HSV-1 contains 2,205 bases between the putative cap site at base 195 and the *Sma*I site at base 2400. In strain 17*syn*$^+$, this distance is 2,102 bases; this small difference in length of the LATs isolated from mouse ganglia latently infected with the two strains is resolvable on some gels (cf. Fig. 5, lanes ii and iii). There are 15 sites between

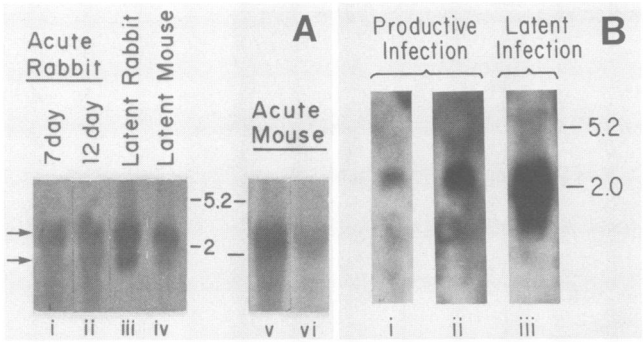

FIG. 4. Detection of spliced LAT in different phases of infection in experimental animals and cultured cells. (A) Acutely infected rabbit and mouse trigeminal ganglia. RNA was isolated from rabbit trigeminal ganglia obtained 7 and 12 days after inoculation (lanes i and ii) and from mouse sensory nerve ganglia 4 days after inoculation (lanes v and vi). For rabbits, RNA from a complete ganglia was fractionated by formaldehyde-agarose gel electrophoresis; for mice, RNA from 50 ganglia was used. RNA was blotted onto membranes and hybridized with LAT-specific probes. Also shown are RNA samples from 1/4 of a latently infected rabbit ganglia (lane iii) or from 15 latently infected mouse ganglia (lane iv). Hybridization probe was a synthetic oligonucleotide spanning bases 1100 to 1120 for lanes i to iv, nick-translated *Sph*I-*Kpn*I DNA (bases 1 to 709) for lane v, and nick-translated *Kpn*I-*Hpa*I DNA (bases 710 to 1036) for lane vi. Nucleotide numbers are as described previously (22). (B) Cultured cells. Cultured rabbit skin cells were infected with a multiplicity of infection of 10 PFU of the KOS(M) strain of HSV-1 per cell either in the presence or absence of 50 μg of cycloheximide per ml. After 5 h, poly(A)$^-$ RNA from 4×10^6 drug-treated cells (lane i) or poly(A)$^-$ RNA from 3×10^6 untreated cells (lane ii) was extracted and fractionated along with total RNA from 20% of a rabbit ganglia latently infected with the McKrae strain of virus. The blots were hybridized with a nick-translated probe spanning the *Kpn*I to *Hpa*I sites shown in Fig. 1 (bases 1 to 709 of the previously published sequence of the KOS(M) strain [22]). The approximate positions of rRNA markers (2.0 and 5.2 kb) are indicated.

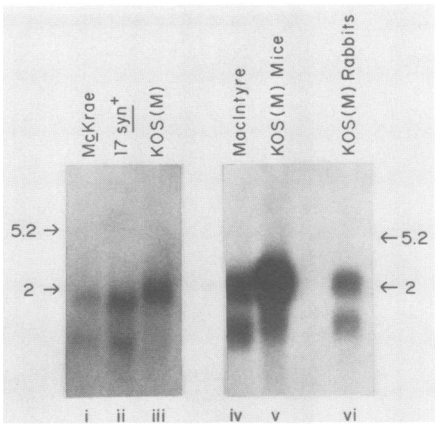

FIG. 5. LAT is spliced with variable efficiency in mouse and rabbit neurons latently infected with different strains of HSV-1. RNA from 15 ganglia from mice latently infected with strain HSV-1 KOS(M) (lanes i and v) or from ganglia of 40 mice latently infected with strains McKrae (lane i), 17*syn*$^+$ (lane ii), MacIntyre (lane iv), and or from a full rabbit trigeminal ganglia latently infected with the KOS(M) strain (lane vi) were fractionated and blotted as described in the experimental section. The blots were hybridized with a nick-translated probe spanning the *Hpa*I to *Sal*I sites shown in Fig. 1 (bases 1207 to 1739 of the published sequence of the KOS(M) strain [22]). The approximate positions of rRNA markers (2.0 and 5.2 kb) are indicated.

the LAT 5′ terminus and the beginning of the major translational reading frame (ORF2) in which there are either base changes or differences in the number of bases encoded. A total of 12 of these differences are within the intron (bases 300 to 1034); however, only one change was seen near the splice donor and acceptor sites. This change is at base 320 where the GTTATTTT in the KOS(M) strain is GTTCTTTT in strain 17*syn*$^+$. Which of these base changes is the cause of the strain differences seen is unclear, and we have not characterized them further at this time.

There is no readily detectable poly(A)$^+$ LAT species in latently infected neurons. The fact that LAT is processed in the latent phase of infection makes it quite important to fully characterize the 3′ portion of the transcript. Although, as we reported earlier (22), very small amounts of an RNA species of a size indistinguishable from the 2.3-kb species could be detected with difficulty in the poly(A)$^+$ RNA from latently infected mouse sensory nerve ganglia, the careful analysis described below strongly indicated that LATs in the poly(A)$^+$-containing fractions of RNA from latently infected mouse and rabbit ganglia result from contamination of these fractions and are not attributable to specific polyadenylated LAT species.

This conclusion was based on the results of several types of control experiments. First, as shown in Fig. 6, although small amounts of LAT could occasionally be recovered in the poly(A)$^+$-containing fractions of RNA isolated from latently infected rabbit and mouse trigeminal ganglia by our standard methods of oligo(dT) chromatography, careful refractionation of the poly(A)$^+$-containing RNA by repassage through oligo(dT)-cellulose resulted in the loss of any detectable LAT signal from the poly(A)$^+$ fraction. Second, when

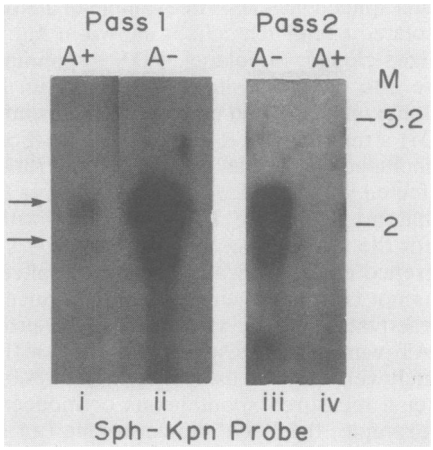

FIG. 6. Lack of detectable LAT in the poly(A)$^+$ RNA fraction isolated from latently infected rabbit trigeminal ganglia. Pass 1, Total LAT RNA from one trigeminal ganglia was passed through 50 mg of oligo(dT)-cellulose and rinsed according to the standard methods described in the experimental section. All of the poly(A)$^+$ and 25% of the poly(A)$^-$ fractions were then fractionated in parallel on a formaldehyde-containing agarose gel and blotted onto nylon membranes. Pass 2 shows results of a similar experiment in which the total poly(A)$^+$ RNA from a first passage through oligo(dT)-cellulose was refractionated with a second 50-mg quantity of oligo(dT)-cellulose; the poly(A)$^-$-containing RNA was then fractionated in parallel with the same amount of poly(A)$^-$ RNA from a single pass as that shown in pass 1. Both blots were then hybridized with 40×10^6 cpm of ^{32}P-labeled *Sph*I-*Kpn*I DNA covering bases 1 to 700 of the previously published sequence (22). Exposure was for 16 h at −70°C, using DuPont Cronex intensifying screens.

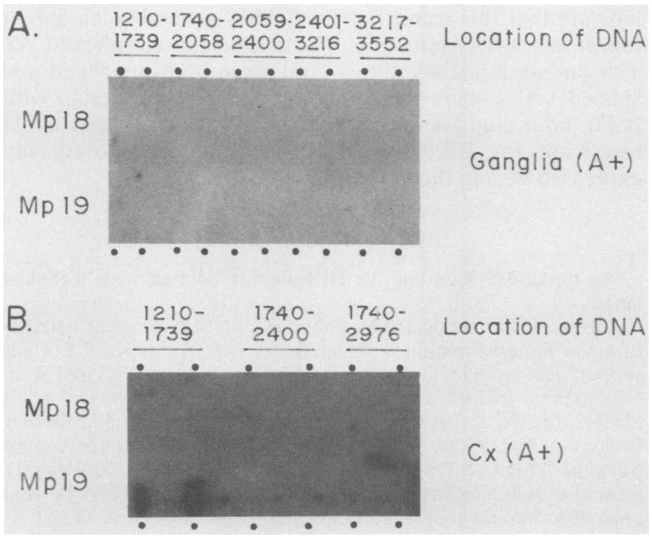

FIG. 7. Latently infected ganglia poly(A)$^+$ RNA does not allow the synthesis of oligo(dT)-primed cDNA hybridizing to HSV DNA around the terminus of the poly(A)$^-$ transcripts. (A) Total poly(A)$^+$ RNA from one latently infected rabbit trigeminal ganglia (equivalent to pass 2 of Fig. 6) was used for oligo(dT)-primed cDNA synthesis as described in Materials and Methods. Here, 12 × 10^6 cpm of ^{32}P-labeled DNA fragments were hybridized with the blot shown. DNA fragments were from the *Hpa*I-*Sal*I site (0.785 to 0.790 m.u.) (bases 1210 to 1739), the *Sal*I-*Sau*3A site (bases 1740 to 2058), the *Sau*3A-*Sma*I site (bases 2059 to 2400), the *Sma*I-*Nae*I site (bases 2401 to 3216), and the *Nae*I-*Kpn*I site (bases 3217 to 3552). Sequence numbers are as given in reference 22 and in Table 1. Single-stranded DNA was cloned in M13 bacteriophage. Exposure was for 4 days with intensifying screens. (B) As a control experiment, 8 μg of poly(A)$^+$ RNA from cycloheximide-treated rabbit skin cells infected with the KOS(M) strain of HSV-1 was used for oligo(dT)-primed cDNA synthesis as described above; the RNA was hybridized with single-stranded HSV-1 DNA covering the 3′ ends of both ICP0 mRNA and LAT. In the experiment shown, 8 × 10^6 cpm of ^{32}P-labeled DNA fragments were hybridized and exposure was for 16 h with intensifying screens.

LAT was detected in the poly(A)$^+$-containing fraction of latently infected ganglia RNA, it was always the same size as LAT in the corresponding and much more abundant poly(A)$^-$ species (cf. Fig. 6, lanes i and ii). This identity of migration rate was also seen by another group (17). Since, in general, polyadenylation requires the addition of an average of 200 A residues for most mRNAs (2, 13, 20), such identity of size would require that a splice within the body of the mRNA exactly compensate for the extra nucleotides.

We also carried out the synthesis of oligo(dT)-primed cDNA, using the total or the poly(A)$^+$ fraction of latently infected rabbit ganglia RNA, and hybridized this radioactive material to single-stranded DNA probes spanning the region between the *Hpa*I site at 0.785 map units (m.u.) to beyond the *Bam*HI site at 0.807 m.u. All attempts failed to show evidence of specific hybridization to any of these probes. When radioactivity was detected hybridizing to probe DNA, it was not confined to the proper DNA strand for LAT (data not shown), and we concluded that the hybridization was an artifact. DNA within the region spanning the *Kpn*I to *Bam*HI sites was especially prone to such artifactual hybridization when it was seen. Figure 7A shows one example of several experiments in which no hybridization could be seen to any region of the DNA tested. Control experiments shown in Fig. 7B, using oligo(dT)-primed cDNA synthesized complementary to poly(A)$^+$ RNA from cycloheximide-treated, infected cells showed strong hybridization to the strand of the *Hpa*I-*Sal*I fragment complementary to the 3′ end of ICP0 (near base 1550), as was expected.

TABLE 1. Sequence differences between the KOS(M) and 17*syn*$^+$ strains of HSV-1 within the sequence of the ICP0 gene beyond the LAT open reading frame[a]

Nucleotide no. in strain:		Difference[b]	Effect ICP0 protein
KOS(M)[c]	17*syn*$^+$		
3500	2112	G to T	None
3442	2170	A to G	None (in intron 2)
3430–3431	2196–2198	Delete AGG	None (in intron 2)
3384–3387	2227	Add GGGC	None (in intron 2)
3156	2455	C to T	None
3100	2511	C to T	None
3071–3072	2540–2552	Delete $G_4T_2G_4T_2$	GGVGVGVG to GGVG
2895	2728	G to T	None
2868	2755	A to C	None
2835	2788	C to T	None
2829	2794	A to G	None
2779	2844	C to G	P to R
2665	2958	C to G	S to W
2640	2983	G to A	None
2585–2598	3024–3025	Add $TC_2G_3CGC_7$	APLP to APPGAPPLP
2407	3202	T to A	None

[a] Data for strain 17*syn*$^+$ is from Perry et al. (14).
[b] Changes shown are from the ICP0 sense strand of the 17*syn*$^+$ strain to the ICP0 sense strand of the KOS(M) strain.
[c] Numbering continues from base 2400 of the previously published sequence (22).

Finally, we have continued our sequence analysis of the DNA of the KOS(M) strain 3′ of the major transcription terminus of LAT which occurs near the *Sam*I site at 0.794 m.u. (base 2400 in our previously published sequence [22]). Differences between the KOS(M) strain and the published sequence for the 17*syn*$^+$ strain of HSV-1 in the 1,200 bases 3′ of the *Sma*I site are shown in Table 1. As in the 17*syn*$^+$ strain, the only variant on a consensus poly(A) addition signal is seen near the *Kpn*I site at 0.802 m.u. This is the sequence AGATAAA 1,173 bases beyond the *Sma*I site at 0.794 m.u. No significant hybridization of oligo(dT)-primed cDNA synthesized from latently infected rabbit ganglia poly(A)$^+$ RNA was seen hybridizing to DNA in this region of the genome (Fig. 7A). Taken together, these data present strong evidence that LAT is not polyadenylated in the latent phase of infection in either rabbit or mouse neurons.

DISCUSSION

The data presented here demonstrate that expression of the HSV-1 LAT is accompanied by a splicing event following establishment of the latent phase of infection in mouse or rabbit neurons (Fig. 1 and 4A). Although further experimental study is currently underway to fully characterize this splice, the correlation between oligonucleotide mapping and nuclease protection experiments locates the intron within the limits of bases 297 and 1033 of the previously published sequence (22). This resolution is adequate to locate the intron outside the major open translational frame characterized from those sequence data.

Recently, another laboratory has also shown that expression of the smaller LAT species is a consequence of the establishment of the latent phase of infection; however, the

splice reported here was not characterized (18). Further support for our conclusion that splicing of the LAT is a consequence of latent infection comes from the point that although unspliced poly(A)$^-$ LAT is detectable at low levels during productive infection of cultured cells, we found no evidence for the presence of the spliced species under these conditions (Fig. 4B).

Although it is clear from the data presented in Fig. 5 that LATs expressed by different strains of HSV-1 differ in either the efficiency of splicing or the stability of the spliced transcript following the establishment of latency in mice, the data from rabbits indicate that the species of animal in which the latent infection is established is also very important. Since all strains of virus examined here establish latent infections in mice, it follows that the relative proportion of spliced LAT observed does not correlate with the establishment of latency per se.

Although we have not yet correlated the splicing of LAT in the latent phase of infection with any particular stage of latency, the fact that it is an indicator of the latent phase of infection suggests that it has a biologically important function. As published earlier (22), we analyzed the sequence of the DNA encoding LAT and found only one large translational reading frame. It is clear that the splice characterized in this communication positions this large open reading frame within 250 bases of the transcript start site. A simple interpretation of such a result is that the splice provides a translational leader length well within the limits of those characterized for other HSV mRNAs. This and the fact that there is little sequence divergence in this open reading frame in two strains of HSV-1 (14, 22) makes it tempting to speculate that a function of the spliced LAT is to encode a protein. Of course, our data do not rule out other physiological roles for the processing observed.

The close correlation with our RNA blot mapping data and the sequence analysis reported previously (22) indicates that the intron characterized in Fig. 1 and 2 is the only major one within the LAT. We have used oligonucleotides 3′ of the splice acceptor site at base 1030 to scan the 3′ region of the LAT to determine whether there were any further small introns detectable. All probes tested within the region from bases 1100 through 2400 hybridized with reasonable efficiency to both the spliced and unspliced species of LAT (data not shown). From this we conclude that there are no other readily detectable introns 3′ of the one characterized here.

We carried out the extensive control experiments described above in order to rigorously characterize any possible poly(A)$^+$ species of HSV LATs. We did this not only because of our own ability to recover very small amounts in the poly(A)$^+$ fraction from a first oligo(dT)-cellulose column, but also because two other laboratories have reported data suggesting the possibility of such a species (15, 17). Although we cannot conclusively rule out a poly(A)$^+$ LAT fraction below reasonable levels of detection, it is more likely that the occasional isolation of the LAT in the poly(A)$^+$ fraction is due to inefficient fractionation. It is also clear that any polyadenylation of the LAT in the latent phase of infection in mouse or rabbit neurons is below our limits of detection, and LAT is retained in the nucleus of the latently infected cells. This suggests that any protein encoded by it must be expressed either at very low levels or at a very temporally restricted phase in the cycle of HSV latency and reactivation.

In conclusion, it may be noted that the occurrence of a spliced species of LAT in latently infected neurons could indicate that this transcript family has several roles during this phase of HSV infection. We have discussed spliced LAT as a potential mRNA above, and since both unspliced and spliced LATs share the same complementary overlap with ICP0, both could serve as anti-sense regulators that could inactivate any ICP0 transcript that might be sporadically expressed during the latent phase.

ACKNOWLEDGMENTS

We thank M. Rice and V. Dissette for helping with technical details.

This work was supported by Public Health Service grant AI06286 from the National Institutes of Health to J.G.S. and E.K.W. Further support was provided by Public Health Service grant CA11861 from the National Institutes of Health, American Cancer Society grant MV372, the UC Irvine Focused Research Program in the Molecular Biology of Eucaryotic Viruses (E.K.W.), Multiple Sclerosis grant RG-1647-A1 (J.G.S.), and Public Health Service grant EY EY06311 from the National Institutes of Health to J.M.H. W.M.F. is a predoctoral trainee of a carcinogenesis training grant (T32-CA-09054).

LITERATURE CITED

1. **Berman, E. J., and J. M. Hill.** 1985. Spontaneous ocular shedding of HSV-1 in latently infected rabbits. Invest. Opthalmol. Visual Sci. **26**:587–590.
2. **Birnstiel, M., M. Busslinger, and K. Strub.** 1985. Transcription termination and 3′ processing: the end is in site! Cell **41**:349–359.
3. **Cox, K. H., D. V. DeLeon, L. M. Angerer, and R. C. Angerer.** 1984. Detection of mRNAs in sea urchin embryos by *in situ* hybridization using asymmetric RNA probes. Dev. Biol. **101**: 485–502.
4. **Croen, K. D., J. M. Ostrove, L. J. Dragovic, J. E. Smialek, and S. E. Straus.** 1987. Latent herpes simplex virus in human trigeminal ganglia. N. Engl. J. Med. **317**:1427–1432.
5. **Denhardt, D. T.** 1966. A membrane-filter technique for the detection of complementary DNA. Biochem. Biophys. Res. Commun. **23**:641–646.
6. **Draper, K. G., G. B. Devi-Rao, R. Costa, E. Blair, R. L. Thompson, and E. Wagner.** 1986. Characterization of the genes encoding herpes simplex virus types 1 and 2 alkaline exonuclease and overlapping proteins. J. Virol. **57**:1023–1036.
7. **Hill, J. M., Y. Haruta, and D. S. Rootman.** 1987. Adrenergically induced recurrent HSV-1 corneal epithelial lesions. Curr. Eye Res. **6**:1065–1071.
8. **Holland, L. E., K. P. Anderson, J. R. Stringer, and E. K. Wagner.** 1979. Isolation and localization of herpes simplex virus type 1 mRNA abundant before viral DNA synthesis. J. Virol. **31**:447–462.
9. **Inoue, T., and T. R. Cech.** 1985. Secondary structure of the circular form of the tetrahymena rRNA intervening sequence: a technique for RNA structure analysis using chemical probes and reverse transcriptase. Proc. Natl. Acad. Sci. USA **82**:648–652.

9a. **Javier, R. T., V. B. Dissette, E. K. Wagner, and J. G. Stevens.** 1988. A herpes simplex virus transcript abundant in latently-infected neurons is dispensible for establishment of the latent state. Virology **166**:254–257.

10. **Maniatis, T., E. F. Fritsch, and J. Sambrook.** 1982. Molecular cloning: a laboratory manual, pp. 109–121. Cold Spring Harbor Laboratory, Cold Spring Harbor, N.Y.
11. **McPheeters, D. S., A. Christensen, E. T. Young, G. Stormo, and L. Gold.** 1986. Translational regulation of expression of the bacteriophage T4 lysozyme gene. Nucleic Acids Res. **14**:5813–5826.
12. **Messing, J., and J. Vieira.** 1982. A new pair of M-13 vectors for selecting either DNA strand of double-digest restriction fragments. Gene **19**:269–276.
13. **Nevins, J. R., and J. E. Darnell.** 1978. Steps in the processing of Ad2 mRNA: poly(A)$^+$ nuclear sequences are conserved and poly(A) addition precedes splicing. Cell **15**:1477–1493.

14. **Perry, L. J., F. J. Rixon, R. D. Everett, M. C. Frame, and D. L. McGeoch.** 1986. Characterization of the IE 110 genes of herpes simplex virus type 1. J. Gen. Virol. **67**:2365–2380.
15. **Puga, A., and A. L. Notkins.** 1987. Continued expression of a poly(A)$^+$ transcript of herpes simplex virus type 1 in trigeminal ganglia of latently infected mice. J. Virol. **61**:1700–1703.
16. **Rock, D. L., A. B. Nesburn, H. Ghiasi, J. Ong, T. L. Lewis, J. R. Lokensgard, and S. L. Wechsler.** 1987. Detection of latency-related viral RNAs in trigeminal ganglia of rabbits latently infected with herpes simplex virus type 1. J. Virol. **61**:3820–3826.
17. **Spivack, J. G., and N. W. Fraser.** 1987. Detection of herpes simplex virus type 1 transcripts during latent infection in mice. J. Virol. **61**:3841–3847.
18. **Spivack, J. G., and N. W. Fraser.** 1988. Expression of herpes simplex virus type 1 latency-associated transcripts in the trigeminal ganglia of mice during acute infection and reactivation of latent infection. J. Virol. **62**:1479–1485.
18a. **Stevens, J. G., L. Haarr, D. D. Porter, M. L. Cook, and E. K. Wagner.** 1988. The herpes simplex virus latency associated transcript is prominent in trigeminal ganglia for seropositve humans. J. Infect. Dis. **158**:117–122.
19. **Stevens, J. G., E. K. Wagner, G. B. Devi-Rao, M. L. Cook, and L. Feldman.** 1987. RNA complementary to a herpesvirus alpha gene mRNA is predominant in latently infected neurons. Science **235**:1056–1059.
20. **Stringer, J. R., L. E. Holland, R. I. Swanstrom, K. Pivo, and E. K. Wagner.** 1977. Quantitation of herpes simplex virus type 1 RNA in infected HeLa cells. J. Virol. **21**:889–901.
21. **Thompson, R. L., M. L. Cook, G. B. Devi-Rao, E. K. Wagner, and J. G. Stevens.** 1986. Functional and molecular analyses of the avirulent wild-type herpes simplex virus type 1 strain KOS. J. Virol. **58**:203–211.
22. **Wagner, E. K., G. Devi-Rao, L. T. Feldman, A. T. Dobson, Y.-F. Zhang, W. M. Flanagan, and J. G. Stevens.** 1988. Physical characterization of the herpes simplex virus latency associated transcript in neurons. J. Virol. **62**:1194–1202.
23. **Zhang, Y.-F., G. Devi-Rao, M. Rice, R. Sandri-Goldin, and E. Wagner.** 1987. Effect of elevated levels of HSV alpha gene products on the expression of model early and late genes *in vivo*. Virology **157**:99–106.